

On the classical reaction rate and the first-time problems of Brownian motion

Aihua Zhang^{1,*} and Sun Choi^{1,†}

¹*Global AI Drug Discovery Center, College of Pharmacy and Graduate School of Pharmaceutical Sciences, Ewha Womans University, Seoul 03760, Republic of Korea*

(Dated: May 9, 2023)

We have developed efficient techniques to solve the first-time problems of Brownian motion. Based on a time-scale separation of recrossings, we show that Eyring's transmission coefficient (κ) equals to the one (κ_V) corresponding to an absorbing boundary consistent with the transition state theory, which is greater than the one (κ_K) derived by Kramers. We also propose methods for reaction rate determination by analyzing short-time trajectories from the barrier maximum, and discuss the relation to the reactive flux method and the significance of reaction coordinates.

In 1940, Kramers published a seminal paper [1] in which he derived the expressions of transmission coefficients (κ_K) of thermally activated barrier crossing from a Brownian motion model of chemical reactions. The development in the following fifty years had been thoroughly reviewed by Hänggi et al. [2] and a brief history of reaction rate theory was presented by Pollak and Talkner [3] a century after Einstein's work on Brownian motion [4]. Kramers' derivation was performed separately for the cases of very weak friction and moderate-to-strong damping. In this work, we focus on the latter case and show that κ_K corresponds to the survival probability ($\lim_{t \rightarrow \infty} \Phi_K(t)$) for an ensemble of systems having crossed the barrier maximum never to recross a specific absorbing boundary involving both the reaction coordinate (q) and its conjugate momentum (p). We then work on a transmission coefficient (κ_V) for an absorbing boundary specified only in q and consistent with the transition state theory (TST) [5], which is intimately related to the recurrence time problem of Brownian motion mentioned by Wang and Uhlenbeck [6] or the distribution of zero-crossing intervals of random processes referred to in the mathematical literature [7]. We develop efficient techniques to determine κ_V and related $\Phi_V(t)$. Based on a time-scale separation of recrossings, we find that Eyring's transmission coefficient (κ) [8] can be interpreted as κ_V , which is greater than κ_K . In the end, we propose methods to calculate reaction rates by short-time simulations starting from the barrier maximum, and discuss the relation to the reactive flux method and the importance of reaction coordinates. In appendix, we demonstrate that the technique can also be applied to the first passage time (FPT) problem of Brownian motion.

Following Kramers' treatment, we start with the familiar Langevin equation for Brownian motion in a force field, i.e.

$$m\ddot{q} + \gamma\dot{q} + U'(q) = \xi(t), \quad (1)$$

where each overdot denotes a derivative with respect to time, m the effective mass, γ the friction coefficient and $U(q)$ the potential of mean force (PMF) for an elementary reaction along the reaction coordinate. We assume

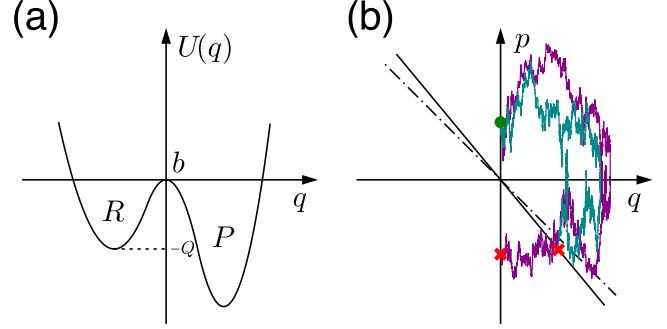


FIG. 1. (a) A schematic graph of the PMF of an elementary reaction. (b) Example random trajectories that stop at the absorbing boundary K (cyan) and V (purple).

a canonical ensemble and $\xi(t)$ is Gaussian white noise of zero mean with the correlation function being

$$\langle \xi(t)\xi(s) \rangle = 2\gamma k_B T \delta(t-s),$$

where $\langle \cdot \rangle$ stands for canonical ensemble average, k_B the Boltzmann constant, T the temperature and $\delta(\cdot)$ the Dirac function. We take the reaction coordinate as a *predefined* dynamical variable coupled to some measuring process, by which locally stable reactant ($q < 0$) and product ($q > 0$) can be distinguished. The dividing surface ($q = 0$) is naturally chosen at the barrier maximum of $U(q)$, i.e. the least probable configuration [9]. A schematic graph of $U(q)$ is shown in Fig. 1(a). In the following, we will change units so that $\gamma = m = k_B T = 1$ and especially, the time unit will be m/γ . We assume that around the barrier maximum and the reactant minimum ($q = -L$), $U(q)$ can be approximated as

$$U(q) = \begin{cases} -\frac{1}{2}\omega_b^2 q^2 & q \sim b \\ \frac{1}{2}\omega_R^2 (q+L)^2 - Q & q \sim R, \end{cases} \quad (2)$$

where Q is the barrier height. With the system in thermal equilibrium, the forward flux ($R \rightarrow P$) through the dividing surface and the reactant population can be calculated by $j^+ = \langle p \theta(p) \delta(q) \rangle$ and $n_R = \langle \theta(-q) \rangle$ ($\theta(\cdot)$ is the Heaviside function), respectively. By the flux-over-population

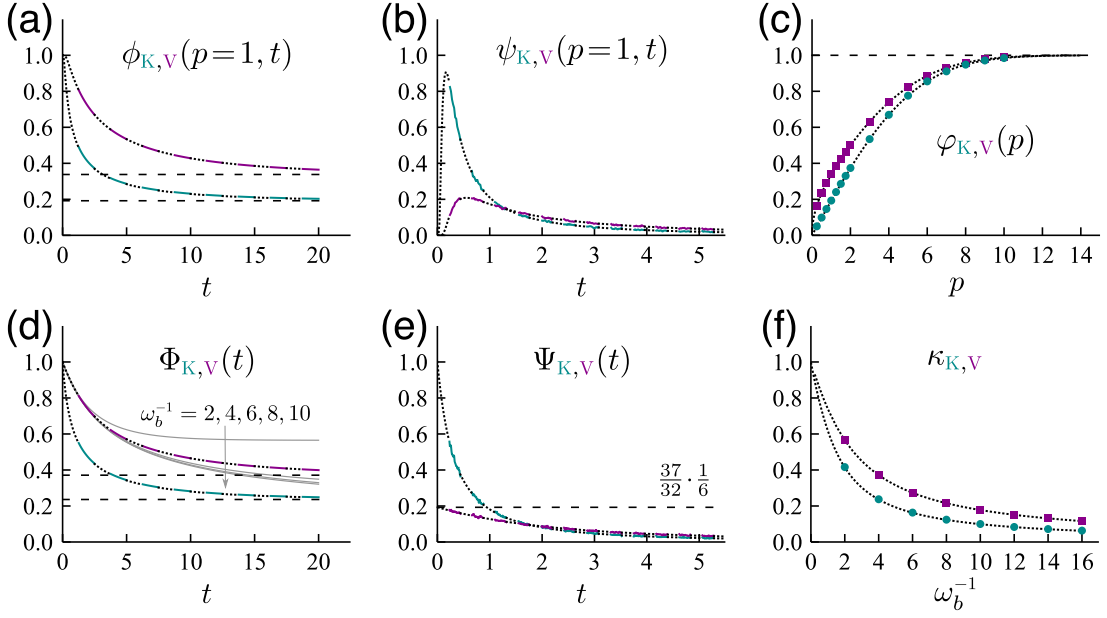


FIG. 2. (a) p -resolved survival probabilities up to time t . (b) p -resolved probability densities of recrossing at time t . (c) p -resolved probabilities of never-recrossing. (d) j^+ -averaged survival probabilities up to time t . (e) j^+ -averaged probability densities of recrossing at time t . (f) Transmission coefficients. The solid (dotted) curves or scattered symbols correspond to simulated (calculated) data. The cyan (purple) curves are for the boundary K (V). Curves in (a-e) are generated with $\omega_b^{-1} = 4$. Φ_V -curves for other ω_b^{-1} values are shown as gray in (d). The calculated and simulated curves are plotted alternatively for clarity.

method [10], the classical TST rate is obtained as

$$k_{\text{TST}} = \frac{j^+}{n_R} \approx \frac{\omega_R}{2\pi} e^{-Q}. \quad (3)$$

However, k_{TST} overestimates the actual reaction rate (k) and an *ad hoc* fudge factor (κ) was introduced by Eyring to account for the discrepancy, which was attributed to the system's recrossing the dividing surface, i.e.

$$k = \kappa \cdot k_{\text{TST}}. \quad (4)$$

Since recrossing eventually happens in an equilibrium, this hints at a problem of time-scale separation.

If we define $a_{\pm} \equiv (\sqrt{1 + 4\omega_b^2} \pm 1)/2$, then Kramers' transmission coefficient has the form of $\kappa_K = \sqrt{a_-/a_+}$. The fact that κ_K depends only on ω_b implies that it is related to dynamics around the barrier maximum, for which the Langevin equation is reduced to

$$\ddot{q} + \dot{q} - \omega_b^2 q = \xi(t). \quad (5)$$

The Kolmogorov backward equation [11] corresponding to Eq. (5) reads

$$\phi_t = (\omega_b^2 q - p)\phi_p + p\phi_q + \phi_{pp}, \quad (6)$$

where each subscript denotes a partial derivative, and $\phi(q, p, t)$ is the probability that a representative point initially situated at (q, p) survives from hitting an absorbing boundary for the time up to t . If $\phi = \phi(u, t)$ and

$u = p + a_+ q$, the problem is further simplified to

$$\phi_t = a_- u \phi_u + \phi_{uu}, \quad (7)$$

which can be solved by

$$\phi_K(u, t) = \text{erf}(\sqrt{a_-(1 + \coth(a_- t))} u/2) \quad (8)$$

for the initial condition, $\phi(u, 0) = \theta(u)$, and the absorbing boundary condition, $\phi(0, t) = 0$. As a result, with an absorbing boundary set up at $p + a_+ q = 0$ (K), the probability of no-recrossing up to t for a system crossing the dividing surface with momentum p will be $\phi_K(p, t)$, i.e.

$$\phi_K(p, t) = \text{Pr}\{p(\tau) + a_+ q(\tau) > 0 \text{ for } 0 < \tau \leq t \mid q(0) = 0, p(0) = p\}. \quad (9)$$

An example random trajectory in the phase space that starts from $(0, 1)$ and ends at the boundary K is shown in Fig. 1(b). Since the inverted harmonic potential in Eq. (5) extends to negative infinity, there is a finite probability of never-recrossing, i.e. $\varphi_K(p) \equiv \lim_{t \rightarrow \infty} \phi_K(p, t) > 0$. The average survival probability for the ensemble of the equilibrium forward flux j^+ can be calculated by $\Phi_K(t) = \langle \phi_K(p, t) \rangle_{j^+} \equiv \langle \phi_K(p, t) p \theta(p) \delta(q) \rangle$, which gives the result of

$$\Phi_K(t) = \sqrt{\frac{a_-}{a_+ - e^{-2a_- t}}}. \quad (10)$$

It is easy to see $\kappa_K = \Phi_K(\infty)$, by which κ_K can be interpreted as the fraction of j^+ that will never recross the boundary K on the infinite inverted harmonic potential. The p -resolved and j^+ -averaged probability density of recrossing time can be easily obtained by $\psi_K(p, t) = -\dot{\phi}_K(p, t)$ and $\Psi_K(t) = -\dot{\Phi}_K(t)$, respectively. Curves of ϕ_K , ψ_K , φ_K , Φ_K and Ψ_K calculated for $\omega_b^{-1} = 4$ are shown in Fig. 2(a-e), and κ_K as a function of ω_b^{-1} is presented in Fig. 2(f). All calculated data agree with the results analyzed according to Eq. (9) from trajectories simulated by integrating Eq. (5) using the BAOAB algorithm [12] with a time step of 10^{-4} .

We proceed to solve the same problem but with a perpendicular absorbing boundary set up at $q=0$ (V), which is consistent with the dividing surface for the transition state theory. An example random trajectory that starts from $(0, 1)$ and recrosses $q = 0$ with $p < 0$ is shown in Fig. 1(b). A fundamental property of the random trajectories in the phase space is that any recrossing through $q = q_0$ takes place by winding around the point of $(q_0, 0)$ [13]. If a system starts from (q_0, p_0) , evolves according to Eq. (5) for time t and arrives at (q, p) , there exists an analytic expression [14] for the transition probability density (TPD), $\varrho(q, p, t; q_0, p_0)$. Suppose a system starts from $q = 0$ with $p > 0$ or $p_0 > 0$. Let $\varphi_V(p)$ denote the probability of no-recrossing, $\tilde{\varphi}_V(p_0)$ the probability of eventually staying in $q > 0$, i.e.

$$\tilde{\varphi}_V(p_0) = \lim_{t \rightarrow \infty} \int_{-\infty}^{\infty} dp \int_0^{\infty} dq \varrho(q, p, t; 0, p_0),$$

and $\mathbb{F}(p_0, p)dp$ the probability of winding back through $(p, p + dp)$, i.e.

$$\mathbb{F}(p_0, p) = \int_0^{\infty} dt p \varrho(0, p, t; 0, p_0).$$

Then we can decompose $\tilde{\varphi}_V(p)$ into cases of no-recrossing and even-times recrossing as

$$\tilde{\varphi}_V(p_0) = \varphi_V(p_0) + \int_0^{\infty} dp \mathbb{F}(p_0, p) \varphi_V(p). \quad (11)$$

By discretizing the above equation and solving the resulted system of linear equations, we obtain $\varphi_V(p)$ and determine the transmission coefficient for the boundary V by $\kappa_V = \langle \varphi_V(p) \rangle_{j^+}$.

We can also use the fundamental winding property to derive the recrossing time distributions up to a finite time. We assume $p > 0$ and $p_0 > 0$ as before. First, we simplify the notations for the same-place TPD at $q = 0$ by defining $\rho^{\pm}(p, t; p_0) \equiv \varrho(0, \pm p, t; 0, p_0)$. Then we construct a winding operator (\odot) that acts on two successive TPDs of ρ^i and ρ^{ii} , and produces the compounded TPD:

$$\rho^{ii} \odot \rho^i \equiv \int_0^{\infty} dp' \int_0^t dt' \rho^{ii}(p, t-t'; p') p' \rho^i(p', t'; p_0). \quad (12)$$

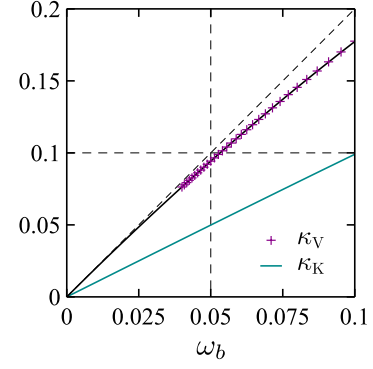


FIG. 3. Asymptotic behaviours of κ_V and κ_K at the diffusive limit ($\omega_b \rightarrow 0$). Numerical values of κ_V can be well fitted with $1.998 \omega_b - 2.249 \omega_b^2$ (the solid black line).

The winding operator is associative but not commutative, and the involved time convolution can be numerically performed using a fast Fourier transform algorithm. Let ζ_1 be similarly defined as ρ^- but for the first-time arrival. Since ρ^- and ρ^+ represent the odd-times and even-times arrivals, respectively, we have a relation of

$$\zeta_1 = \rho^- - \zeta_1 \odot \rho^+. \quad (13)$$

By substituting the above relation into itself recursively, we obtain a series representation of ζ_1 as

$$\zeta_1 = \rho^- - \rho^- \rho^+ + \rho^- \rho^{+2} - \rho^- \rho^{+3} + \dots, \quad (14)$$

where the winding operator is implied between neighboring TPDs. By discretizing ρ^{\pm} and performing a certain number (n) of iterations, 2^n terms of Eq. (14) can be accumulated until achieving a converged ζ_1 , from which the survival probability of $\phi_V(p, t)$ similarly defined as in Eq. (9) can be derived as

$$\phi_V(p, t) = 1 - \int_0^t dt' \int_0^{\infty} dp' p' \zeta_1(p', t'; p). \quad (15)$$

Other functions of ψ_V , Φ_V and Ψ_V follow similarly from ϕ_V as their K counterparts, and are shown together with φ_V and κ_V in Fig. 2, which manifests that all calculated curves for the boundary V also agree with the simulated ones. We can see $\kappa_V > \kappa_K$ in Fig. 2(f), which is consistent with the relative position of K and V boundaries. It is worthy to note that $\Psi_V(0^+)$ equals to the product of the magic number $(37/32)$ derived by Wong [15, 16] and the cubic Taylor coefficient $(1/6)$ of the covariance function for Eq. (5) (see Fig. 2(e)). The fact of $\Psi_V(0^+)$ being constant can be related to the asymptotic form of ρ^{\pm} at $t \rightarrow 0$. It is well known that κ_K is asymptotic to ω_b at the diffusive limit (see Eq. (17) in Ref. [1]). We conjecture that $\kappa_V \sim 2\omega_b$ as $\omega_b \rightarrow 0$ by numerical calculation (see Fig. 3).

So far we have studied the dynamics on an inverted harmonic potential, which approximates a barrier maxi-

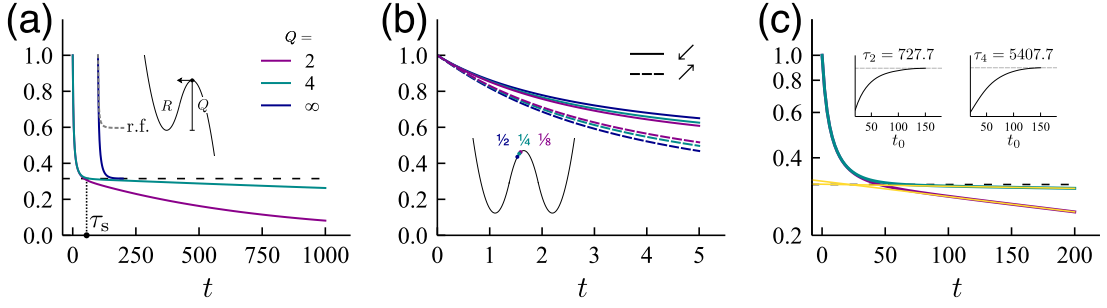


FIG. 4. (a) Φ_V -curves for the backward flux on the inset potential with different barrier heights. The curve labelled by r.f. is calculated by the reactive flux method. The curves for $Q = \infty$ are shifted to right for clarity. (b) The uphill (\nearrow) and downhill (\searrow) Φ_V -curves for different deviations in $k_B T$ away from the barrier maximum of the inset potential. (c) The logarithmic plots of Φ_V -curves for $Q = 2, 4$ in (a) up to a stop time of $t_h = 200$. The insets show the variation of exponential decaying time constants obtained by linear fitting for the interval of $[t_0, t_h]$. The yellow lines correspond to the asymptotic values.

imum with $Q = \infty$. We continue to investigate the dynamics both on a barrier maximum and in a reactant minimum. We model the related $U(q)$ using a differentiable piecewise-quadratic potential (see the inset of Fig. 4(a)), which is parameterized by ω_b , ω_R and Q ($< \infty$). By the flux-over-population formalism for k_{TST} , the transmission coefficient can be understood as a fraction of the forward flux that actually turns into products. On the other hand, k_{TST} is equivalent to the reciprocal of average time that a system in equilibrium spends in the reactant region ($q < 0$). So we can similarly calculate Φ_V and Ψ_V from trajectories for a *backward* flux ensemble, and then k_{TST} can be determined as

$$k_{\text{TST}}^{-1} = \int_0^\infty dt t \Psi_V(t) = \int_0^\infty dt \Phi_V(t). \quad (16)$$

Two example Φ_V -curves with $\omega_b^{-1} = \omega_R^{-1} = 5$ and $Q = 2, 4$ are shown in Fig. 4(a), from which we observe a time-scale separation of recrossings. A $1 - \Phi_V(\tau_s)$ fraction of systems recross in a short time of $t < \tau_s$, while the remaining $\Phi_V(\tau_s)$ fraction of systems are supposed to traverse the minimum and recross in a slowly decaying way. If only the long-time part ($t > \tau_s$) is resolved, the corresponding rate will be

$$k^{-1} = \Phi_V(\tau_s)^{-1} \int_{\tau_s}^\infty dt t \Psi_V(t). \quad (17)$$

If we define $\epsilon = \int_0^{\tau_s} dt (\Phi_V(t) - \Phi_V(\tau_s)) / \int_0^\infty dt \Phi_V(t)$, two rates are related by

$$k = (1 - \epsilon)^{-1} \Phi_V(\tau_s) k_{\text{TST}}. \quad (18)$$

By comparing Φ_V -curves of finite Q with the $Q = \infty$ case (see Fig. 4(a)), we find that the short-time part can be attributed to the dynamics on the barrier maximum, and it is a good approximation to take $\Phi_V(\tau_s) \approx \kappa_V$ even for a small barrier height of $Q = 2$. If $\epsilon \ll 1$ is also the case as in typical conditions, we obtain $k \approx \kappa_V \cdot k_{\text{TST}}$, which establishes an interpretation of κ in Eq. (4) as κ_V .

The above elaboration forms the basis for calculating the reaction rate from simulations started from a barrier maximum. Given a reaction coordinate, the barrier maximum can be determined by symmetry between Φ_V -curves for the forward and backward flux. As shown in Fig. 4(b), a slight deviation of $k_B T/8$ from the barrier maximum will give rise to apparent difference between the uphill and downhill Φ_V -curves. If k_{TST} is available, we only need to simulate $\Phi_V(t)$ up to a short stop time (t_h) less than τ_s . By first scaling the time unit so that $-\Phi_V(0^+)$ matches with $37/192$ and then finding ω_b^{-1} by comparing the resulted curve with Φ_V -curves in Fig. 2(d), we can determine the reaction rate as $\kappa_V k_{\text{TST}}$ after reading out κ_V from Fig. 2(f), and get an estimation of τ_s at the same time. This approach resembles the reactive flux (r.f.) method [17, 18], but the first-time problem is not dealt with in the reactive flux method, and as shown in Fig. 4(a), the corresponding $\Phi_{\text{r.f.}}(t) = \langle \theta(q(t)) \rangle_{j^+}$ overcounts the probability by even-times recrossings.

On the other hand, if the long-time recrossing dynamics obeys the phenomenological exponential decaying [18], i.e. $\Phi_V(t) = \Phi_V(\tau_s) e^{-t/\tau_r}$, we simply have $k \approx \tau_r^{-1}$ by Eq. (17), providing that $\tau_s \ll \tau_r$. In such a case, we can simulate $\Phi_V(t)$ up to $t_h > \tau_s$, and determine the reaction rate by a linear fitting of the long-time part in a logarithmic plot of $\Phi_V(t)$. By fitting Φ_V -curves of $Q = 2, 4$ in Fig. 4(a) up to $t_h = 200$ (see Fig. 4(c)), we obtain $\tau_2 = 727.7$ and $\tau_4 = 5407.7$ for the decaying time constants, which agree with k^{-1} values of 736.9 and 5445.2 calculated using $\kappa_V = 0.315$ for $\omega_b^{-1} = 5$ and k_{TST} from Eq. (3) for $\omega_R^{-1} = 5$. We can roughly estimate the t_h dependence of sampling density by considering the ideal case of $\tau_s \rightarrow 0$. If we start N_s trajectories and let N_r be the number of trajectories that recross at $t > \tau_s$, then the sampling density is approximately constant for a short stop time, i.e. $N_r/t_h \propto N_s$. However, with t_h decreasing, the average recrossing time decreases as t_h^2 , so for a given total simulation time, the sampling density will increase as t_h^{-2} . But in actual cases we can not arbitrarily

decrease t_h due to other considerations.

In his famous paper [19], Zwanzig derived a generalized Langevin equation with $U(q)$ being the PMF for a reaction coordinate (q) from a model Hamiltonian with q coupled bilinearly to a bath of harmonic oscillators ($\{x_i\}$). By suitably choosing the coupling parameters, one can obtain the standard Langevin equation of Eq. (1) in the continuum limit. In the vicinity of the barrier $q \sim 0$, the dynamics of $\{q, x_i\}$ can be decoupled into an unstable normal mode (\tilde{q}) and other modes ($\{\tilde{x}_i\}$) through an orthogonal transformation. Especially, the reaction coordinate q is related to normal modes by $q = c_0 \tilde{q} + \sum c_i \tilde{x}_i$, where c_0 can be assumed positive. Then according to Pollak's work [20], κ_K is simply j_q^+/j_q^- , where j_q^+ and j_q^- are the fluxes through the dividing hyperplane of $q = 0$ and $\tilde{q} = 0$ at the saddle point, respectively. Any trajectory associated with j_q^+ will have $\tilde{q} \rightarrow \infty$, and is necessarily associated with $\kappa_V j_q^+$. However, we have shown that $\kappa_V j_q^+ > \kappa_K j_q^+ = j_q^+$, which indicates that there exist additional trajectories in $\kappa_V j_q^+$ that evolve into the hyperplane of $\tilde{q} = 0$. The above analysis demonstrates that the reaction coordinate determines the very problem of the reaction rate: $k \propto \kappa_V j_q^+$ for q , while $k \propto j_q^+ = \kappa_K j_q^+$ for \tilde{q} . It will underestimate the reaction rate if $j_q^+ = \kappa_K j_q^+$ is used for the reaction coordinate q .

In summary, we have solved the recurrence time problem of Brownian motion on the barrier maximum, and given a rigorous interpretation of the transmission coefficient. We have proposed methods to determine reaction rates by short-time simulations from the barrier maximum, and discussed the relation to the reactive flux method and the significance of reaction coordinates for the reaction rate problem.

This work was supported by the Mid-career Researcher Program (NRF-2020R1A2C2101636), Bio & Medical Technology Development Program (NRF-2022M3E5F3080873), Medical Research Center (MRC) grant (NRF-2018R1A5A2025286), and the Brain Pool Program (NRF-2021H1D3A2A02081370) funded by the Ministry of Science and ICT (MSIT) through the National Research Foundation of Korea (NRF). It was also supported by the Ewha Womans University Research Grant of 2021. We thank T. N. L. Vù for helpful discussions.

Appendix

The winding property can also be used to solve the FPT problem of Brownian motion [6]. What we try to find is the probability density, $\alpha_1(t)$, that a particle starting from (q_i, p_i) passes through $q = q_b$ at time t for the first time. We assume $q_b > q_i$, $p > 0$ and $p_0 > 0$, and define $\rho^\pm(p, t) \equiv \varrho(q_b, \pm p, t; q_i, p_i)$ and $\rho^{\circ, e}(p, t; p_0) \equiv \varrho(q_b, \pm p, t; q_b, -p_0)$ (see inset of Fig. A1). We can similarly determine the first-time probability

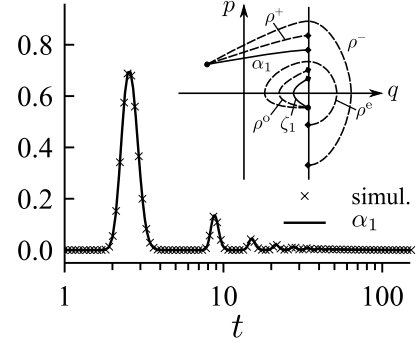


FIG. A1. FPT distributions for the problem studied in Ref. [21]. The inset illustrates the meanings of involved quantities.

density of winding around $(q_b, 0)$, $\zeta_1(p, t; p_0)$, from the relation of $\zeta_1 = \rho^o - \zeta_1 \odot \rho^e$. Then we can calculate the FPT distribution by

$$\alpha_1(t) = \int_0^\infty dp p [\rho^+(p, t) - \zeta_1(p, t; p_0) \odot \rho^-(p_0, t)].$$

We test the approach by solving the problem presented in Sec. III of Ref. [21]. Compared with the FPT distribution calculated up to three terms of the Rice series [22] (Fig. 2 of Ref. [21]), our result is well converged as shown in Fig. A1.

* zah7903@gmail.com

† sunchoi@ewha.ac.kr

- [1] H. A. Kramers, *Physica* **7**, 284 (1940).
- [2] P. Hänggi, P. Talkner, and M. Borkovec, *Rev. Mod. Phys.* **62**, 251 (1990).
- [3] E. Pollak and P. Talkner, *Chaos* **15**, 026116 (2005).
- [4] A. Einstein, *Ann. Phys.* **322**, 549 (1905).
- [5] E. Wigner, *Trans. Faraday Soc.* **34**, 29 (1938).
- [6] M. C. Wang and G. E. Uhlenbeck, *Rev. Mod. Phys.* **17**, 323 (1945).
- [7] I. Blake and W. Lindsey, *IEEE Trans. Inf. Theory* **19**, 295 (1973).
- [8] H. Eyring, *J. Chem. Phys.* **3**, 107 (1935).
- [9] M. G. Evans, *Trans. Faraday Soc.* **34**, 49 (1938).
- [10] L. Farkas, *Z. Phys. Chem.* **125U**, 236 (1927).
- [11] L. Pontryagin, A. Andronov, and A. Vitt, Appendix: On the statistical treatment of dynamical systems, in *Noise in Nonlinear Dynamical Systems*, Vol. 1, edited by F. Moss and P. V. E. McClintock (Cambridge University Press, 1989) p. 329–348.
- [12] B. Leimkuhler and C. Matthews, *Appl. Math. Res. Express* **2013**, 34 (2013).
- [13] H. P. McKean Jr., *J. Math. Kyoto Univ.* **2**, 227 (1962).
- [14] H. Risken, *Solutions of the Kramers Equation, in The Fokker-Planck Equation: Methods of Solution and Applications* (Springer Berlin Heidelberg, Berlin, Heidelberg, 1996) pp. 238–240.
- [15] E. Wong, *SIAM J. Appl. Math.* **14**, 1246 (1966), full publication date: Nov., 1966.

- [16] E. Wong, SIAM J. Appl. Math. **18**, 67 (1970).
- [17] T. Yamamoto, J. Chem. Phys. **33**, 281 (1960).
- [18] D. Chandler, J. Chem. Phys. **68**, 2959 (1978).
- [19] R. Zwanzig, J. Stat. Phys. **9**, 215 (1973).
- [20] E. Pollak, J. Chem. Phys. **85**, 865 (1986).
- [21] T. Verechtchaguina, I. M. Sokolov, and L. Schimansky-Geier, Phys. Rev. E **73**, 031108 (2006).
- [22] S. O. Rice, Bell Syst. Tech. J. **24**, 46 (1945).